

Chapter V

Environmental assessment and nano-mineralogical characterization of raw coal, overburden, and sediment from Ledo coal mining acid drainage area

5.0 Introduction

The NER coals of India pose some unusual physico-chemical features with high organic sulphur and lesser amounts of pyritic and sulphate sulphur (Saikia et al., 2014). Thus, considering the sulphur content, a special importance have been given to the NER coal both in cleaner utilization in power plants and their environmental consequences (Zamuda and Sharpe, 2007). Pyrite mineral in coal is considered to be a host for potentially toxic elements such as As, Hg, Se, Pb, etc. and during the oxidation of the pyrite these elements are found to be released into the environment (Finkelman 1994). The minerals present in coal are very important for geochemical indication of coal. The minerals as well as other inorganic matters associated with coal are the significant factors for evaluating the coal quality in coal mining, preparation, storage, liquefaction, gasification, coking and other important applications (Xiuyi, Mineral Matter in Coal). The mineral matters in coal and overburden are found to be responsible for enormous environmental problems which are being of greater attention. Coals and overburdens are associated with high contents mineral matters which are the noticeable source of various metals and nonmetals. A number of the trace/ hazardous elements associated with the mineral matter of coal and overburden result in environmental degradation by contaminating soil and water resources near coal mining areas (Finkelman, 1995). Generally, the assessment of contamination of hazardous element in soils is carried out by comparing the total concentrations of metals in bulk samples with soil quality standards (SQS) (Ljung et al., 2005, 2006). However, from literature it has been found that the concentrations of various metals in soil increase with decrease in their particle size (Al-Rajahi et al., 1996; Ljung et al., 2006; Hower et al., 2013). The nanoparticles have a specific area for which they can retain high amounts of elements (Wang et al., 2006). Moreover, small particles are easily soluble and can more likely to pass through the gastric mucosa and so more strongly adsorb in human tissues than large fractions (Lin et al., 1998).

Minerals in coal and overburden can occur naturally at nanoscale formed by breakdown processes like weathering and building-up like redox chemical processes (Gaur et al., 2014) From literature (Dutta et al., 2017) it was found that Coal, overburden, soil, sediment, and associated acid mine drainage contain a large amount of nano-minerals. Nano-particles/ nano-minerals and generated during coal processing are found to be responsible for more severe health impacts than larger particles as the nano-particles have can easily enter to life systems through different ways like inhalation, absorption, food chain and ingestion exposure. Once they enter, they circulate in a living organism including human beings causing a number of health problems (Warheit, 2004; Warheit et al., 2003). The nano-particle assemblages results from coal power plants burning can affect the lung cells by mitochondrial impairment, oxidation of proteins, damage to cell membranes by lipid peroxidation, inactivation of enzymes involved in cell metabolism and antioxidant defense and, DNA damage (Schins and Borm, 1999; León-Mejía et al., 2011). Both the processes namely association and stabilization of nano-particles with natural organic material along with other organic contaminants are significant due to their toxicological effects in aquatic ecosystems (Farre et al., 2011). Nano-particles are most normally linked with geological particles /minerals like calcium carbonate, calcium sulphates, quartz, and both Al and Fe-Mg aluminosilicates (Civeira et al., 2016). The stability of nano-minerals has been found to be inversely proportional to their affinity to aggregate (Mackay et al., 2006) and their aggregation power is size dependent (Farre et al., 2011). Moreover, from environmental consideration, one of the most important characteristics of Fe bearing mineral nano-particles like hematite is their high surface area, which enables their role as powerful sequestrants of ions from solution (Silva et al., 2011). Thus, the nano-minerals have the ability to control the mobility of hazardous elements in solution and from different points of view including economic, environmental etc., the mineralogical / nano-mineralogical study of coal and overburden is considered to be very important.

5.1 Methods and materials

The samples that were collected include coal (LC-20A, LC-60A, TC-20A, TC-60A), mine overburden (OB) (LOB-15A, LOB-15B, TOB-15A, TOB-15B), soil (LS-15A, LS-15B, TS-15A, TS-15B) sediment (LSE-15A, LSE-15B). Samples of mine water, seepage water from mining areas, and different water resources namely Ledopani river, Kachanalla stream and Tirap river were randomly collected from the AMD source and within a 5 km radius from the source of the two most active and industrially important coal mines of Makum coalfield namely Ledo and Tirap collieries. The collected sediment, OB and soil samples were air dried, grounded into 0.422 and 0.211 mm size and kept for the analysis. The water samples were preserved for further analysis by adding 10 mL of 1:1 HNO₃ solution. The overburden material, which covers the coal seam, is typically blasted and removed in order to reach the coal seam. This process allows exposure of these materials to physical and chemical weathering, which can release soluble constituents into surrounding water resources (Odenheimer et al., 2015). These samples were collected randomly within the radius of approximately 5 km from the open pit in all directions to find out the impact of coal mining in these areas.

5.2 Experimental sections

5.2.1 Geochemical analyses of solid and water samples

The geochemical analyses of the water samples including pH, TDS, EC analyses were carried out by using relevant instruments and standard methods. The details of the instruments used are explained in chapter II.

5.2.2 Chemical analyses of coal, OB, soil, and sediments

The proximate and C, H, N analysis of coal, soil, sediment and OB samples were carried out with a proximate and elemental analyzers following ASTM methods (ASTM D5373, ASTM D4239). For complete characterization of respective samples different analytical techniques were used including XRD, FTIR, FE-SEM, HR-TEM, Raman, and Mossbauer spectroscopic analyses. The details of the instruments used for these analyses are described in chapter II.

5.2.3 Ion chromatographic analyses of mine / mine affected water

The concentrations of the major ions including both cations (NH_4^+ , Na^+ , K^+ , Ca^{2+} , Mg^{2+}) and anions (F^- , Cl^- , Br^- , SO_4^{2-}) present in mine and mine affected water were determined by ion chromatographic analysis. The complete description of the analytical method is given in chapter II.

5.3 Results and discussions

5.3.1. Geochemical characteristics coal mine water

The geochemical analyses of the water samples collected from the AMD sources of the Ledo and Tirap collieries and different sources including rives, steams and seepage water were performed and the results of geochemical analyses are summarized in Table 5.1. From the analytical data it was found that the pH and EC of water samples vary inversely. The high values of TDS and EC and low values of pH (minimum of 3.3) in the mine rejects and the water samples collected from surrounding areas indicate the dissolution of elements as well as ions. The pH is lowered through production of sulphuric acid by oxidation of pyritic sulphur and other sulfides present in coal and accompanying strata (Baruah et al., 2006). Structural differences and labile sulphur groups present in coal may also indicate low pH. The values of total hardness of water samples including seepage water (TW-15D) and AMD waters (TW-15A, TW-15B) of Tirap colliery are very high compared to Ledo colliery and indicate high possibility of contamination of water resources near Tirap colliery. A high value of water hardness reduces its utility for domestic purposes and increases the life risk for aquatic flora and fauna. It has been noticed that the value of pH of AMD in northeastern coalfield is in similar range with other countries (Chon and Hwang, 2000, Shahabpour et al., 2005). The average pH value for AMD values from Ledo (3.8) and Tirap (3.6) collieries are comparable with the pH value for AMD from coal mines of Jaintia Hills (3.01), Dogye coal mine, Korea (3.7) and Keman coal mine, Iran (3.06).

Table 5.1: Geochemical analysis of water samples

Sample type	Distance from AMD source (km)	pH	Electrical conductivity (ms cm ⁻¹)	Dissolved oxygen (mg/L)	Total dissolved solid (ppt)	Total hardness (mg/L)
Ledo Colliery						
LW-15A	AMD source	4.0	1.23	0.4	Trace	876.0
LW-15B	0.5	4.1	1.23	0.2	Trace	897
LW-15C	0.5	3.5	2.29	0.3	1.14	1276
LW-15D	1	3.3	2.49	0.8	1.18	730
LW-15E	2	4.4	0.94	0.5	Trace	600
LW-15F	5	5.0	0.66	0.2	Trace	460
Tirap Colliery						
TW-15A	AMD source	3.6	3.15	0.3	1.57	2350
TW-15B	1	3.7	2.11	0.4	1.59	2470
TW-15C	0.5	3.5	5.34	0.2	2.65	1350
TW-15D	1.5	3.9	2.11	0.3	1.06	5720

5.3.2 pH of soil, OB, and sediment

Soil pH is not only a nutrient, but it relates to plant nutrition. It controls the availability of plant nutrients. Particular nutrients that a plant needs can exist in the ground in abundance, but for their availability, the nutrients must be soluble. This solubility is affected by soil pH level. Thus, Soil pH is an important measurement as the acidity or alkalinity of soil determines how easily plants can absorb nutrients from it. Plants take up nutrients from soil when the nutrients are dissolved in water. When the soil's pH is too acidic or too alkaline, some of those nutrients – including Fe, N and some other elements are not able to dissolve as proficiently. When soil is too acidic (at a pH less than 6.0), P,

K, and N cannot be properly dissolved and absorbed. When it is too alkaline (at a pH much higher than 7.5), then P, Mn and Fe will not readily soluble in the soil solution. Thus, most plants survive best in soil with a pH value of 6.0 - 7.5 (Beaulieu, 2018). The pH values of soil, overburden, and sediments collected from Ledo and Tirap collieries are mentioned in Table 5.2.

From the Table 5.2, it is found that the pH values of soil, overburden, and sediment samples from Ledo colliery are comparatively low than that of Tirap colliery. According to The United States Department of Agriculture Natural Resources Conservation Service, the classification of soil pH range is as follows (Table 5.3).

Table 5.2: Determination of pH of soil, OB, and sediment of Ledo colliery and nearby Tirap colliery

Sample type	Sample code	pH
Soil	LS-15A	5.25
	LS-15B	5.85
Overburden	LOB-15A	5.65
	LOB-15B	5.43
	TOB-15A	7.25
	TOB-15B	7.40
Sediment	LSE-15A	5.04
	LSE-15B	5.90

Table 5.3: Classification of soil pH range

Denomination	pH range
Ultra acid	3.5
Extremely acidic	3.5-4.4
Very strongly acid	4.5-5.0
Strongly acid	5.1-5.5
Moderately acid	5.6-6.0
Slightly acid	6.1-6.5
Neutral	6.6-7.3
Slightly alkaline	7.4-7.8
Moderately alkaline	7.9-8.4
Strongly alkaline	8.5-9.0
Very strongly alkaline	> 9.0

From Table 5.2 and Table 5.3, it is clear that the soil, OB, and sediment samples are strongly and moderately acidic in nature (5.04-5.90). On the other hand the overburdens from Tirap colliery are almost neutral in nature (pH range 7.25-7.40). Thus the soils near and around Ledo colliery are adversely affected by coal mining activities due to which the soil quality of agricultural areas around the colliery are severely degraded.

5.3.3 Chemical analyses of coal, soil, OB, and sediment

Four different coal samples from the Ledo and Tirap collieries (i.e. LC-20A, LC-60A, TC-20A, TC-60A) were subjected to proximate analysis, and CHNS analysis. The same chemical analyses were also performed for the soil, OB and sediment. The detailed data are summarized in Tables 5.4, 5.5, 5.6, and 5.7. From the proximate analysis, it was found that the coals (from both collieries) have a low moisture and ash contents and high volatile matters. The Meghalaya coal was also found to be low in ash (1.3 to 24.7%), low moisture (0.4-9.2%) and high sulphur (3-5%) (Swier and Singh, 2003) which is comparable to Ledo

and Tirap coal. The CHNS analysis data for coal samples revealed a medium sulphur content with low pyrite and sulphate sulphur and high organically bound sulphur. In coal, forms of sulphur were determined by the standard ASTM method (ASTM D2492-02), and sulphate sulphur was determined through gravimetric method by using the standard BaCl₂ solutions (ASTM D2492-02; Vogel, 1969). Determination of organic sulphur was carried out by subtracting the value of pyrite and sulphate sulphur from the total sulphur. The highest ash content and lowest volatile matter were found in the Ledo colliery samples. However, the sulphur contents in OB, soil and sediment samples are lower than the coals (Table 5.6).

Table 5.4: Proximate analysis of coal (wt %)

Sample code	Moisture content	Volatile matter	Ash content	Fixed carbon
TC-60A	2.07	40.72	2.78	54.43
TC-20A	2.65	40.92	1.78	54.67
LC-60A	3.12	41.27	6.68	48.93
LC-20A	5.33	35.33	19.72	39.63

Table 5.5: CHNS and forms of sulphur analysis of coal (wt %)

Sample code	C	H	N	S _t	S _p	S _s	S _o
TC-60A	80.6	5.88	1.19	3.54	0.61	0.77	2.158
TC-20A	83.3	6.14	1.35	1.94	0.35	0.57	1.02
LC-60A	76.3	5.90	1.02	2.49	0.45	0.69	1.35
LC-20A	73.5	5.05	bdl	2.94	0.49	0.71	1.74

S_t: Total sulphur; S_p: Pyritic sulphur; S_s: Sulphate sulphur; S_o: Organic sulphur

Table 5.6: Proximate analysis of OB, soil and sediment (wt %)

Sample code	Moisture content	Volatile matter	Ash content	Fixed carbon	Total sulphur
LOB-15A	2.55	11.14	89.81	bdl	0.24
LOB-15B	0.82	11.13	91.72	bdl	0.08
TOB-15A	2.69	12.87	86.68	bdl	0.51
TOB-15B	2.17	7.94	93.83	bdl	0.06
LS-15A	0.43	11.18	92.15	bdl	0.04
LS-15B	2.13	9.71	91.96	bdl	0.05
LSE-15A	3.08	11.40	89.08	bdl	0.43
LSE-15B	1.97	12.98	84.65	0.39	0.94

Table 5.7: CHNS analysis of soil, sediment and overburden (wt %)

Sample types	Sample code	C	H	N	S _t
OB	LOB-15A	2.51	1.03	0.17	0.24
	LOB-15B	1.66	0.539	bdl	0.08
	TOB-15A	3.72	1.30	bdl	0.51
	TOB-15B	0.71	0.802	bdl	0.06
Soil	LS-15A	1.36	0.569	bdl	0.04
	LS-15B	1.55	0.911	bdl	0.05
Sediment	LSE-15A	1.92	1.16	0.14	0.43
	LSE-15B	6.84	1.26	0.13	0.94

(C: carbon; H: hydrogen; N: nitrogen)

5.3.4 Ion-chromatographic analyses of mine water/ mine affected water

The concentrations of cations viz. Na^+ , K^+ , Mg^{2+} , Li^+ , NH_4^+ and Pb^{2+} and anions like Cl^- , F^- , SO_4^{2-} and Br^- present in the collected water samples was determined through Ion-chromatographic analysis. Tables 5.8 and 5.9 describe the concentration of cations and anions determined. These tables show is no indication of ammonium ion in mine water, which may be due to the oxidation of ammonium ions into nitrite by aerobic bacteria. On the other hand the water samples of Tirap colliery have high amount of Mg^{2+} ion. The absence of NH_4^+ ion confirms the low pH of water bodies near the mining area. The Tirap samples have very high concentration of Mg^{2+} ion. As the fourth common mineral in our body, Mg is involved in many important biological processes. Mg above the normal range (the normal range for drinking water is 20–30 ppm) can cause severe metabolic disorders like gastrointestinal effects, eczema in children etc. In plants high cytoplasmic Mg^{2+} ion concentration blocks a K^+ ion channel in the inner envelop membrane of the chloroplast, and inhibit the removal of H^+ ions from chloroplast stroma. Very high concentration of Br^- ion occurs in water samples of the Ledo mining area mainly in LW-15A, LW-15D and LW-15F (Table 5.9). The first two were collected from mine water and seepage water. LW-15F sample was collected from Kachanalla River, 5 km away from Ledo colliery. This is an indication of contamination of water bodies even at a longer distance from the source. The high level of Br^- ion giving plasma level of 96 mg/L plasma produces bromism is harmful to the nervous system, skin, glandular secretions and gastrointestinal tract (Leeuwen and Sangster, 1988). Ion-chromatographic analyses of coal, OB, soil and sediment were carried out to identify the presence and amount of ions in these samples which are mentioned on detail in Table 5.10.

Table 5.8: Analysis of cations in coal mine water samples (mg/l)

Cation	LW-15A	LW-15B	LW-15C	LW-15D	LW-15E	LW-15F	TW-15A	TW-15B	TW-15C	TW-15D
Na ⁺	0.559	0.508	0.582	0.531	0.661	0.724	0.480	0.543	0.488	0.881
K ⁺	0.103	0.262	0.301	0.350	1.192	2.137	0.195	0.096	0.164	0.232
Mg ²⁺	44.913	110.25	29.291	35.015	49.781	60.784	242.81	450.05	128.04	240.44

Table 5.9: Analysis of anions in coal mine water (mg/l)

Anion	LW-15A	LW-15B	LW-15C	LW-15D	LW-15E	LW-15F	TW-15A	TW-15B	TW-15C	TW-15D
F ⁻	bdl	0.072	bdl	bdl	bdl	0.864	bdl	bdl	bdl	bdl
Cl ⁻	0.268	1.689	0.741	3.384	0.495	8.846	1.788	1.067	0.675	0.571
Br ⁻	170.10	46.202	66.869	161.41	78.341	227.17	32.764	47.817	52.875	54.988
SO ₄ ²⁻	14.151	8.817	5.496	9.00	3.909	15.408	12.155	15.73	9.974	10.982
NO ₃ ⁻	bdl									

Table 5.10: Ion chromatographic analyses of coal, OB, soil and sediment (mg/l)

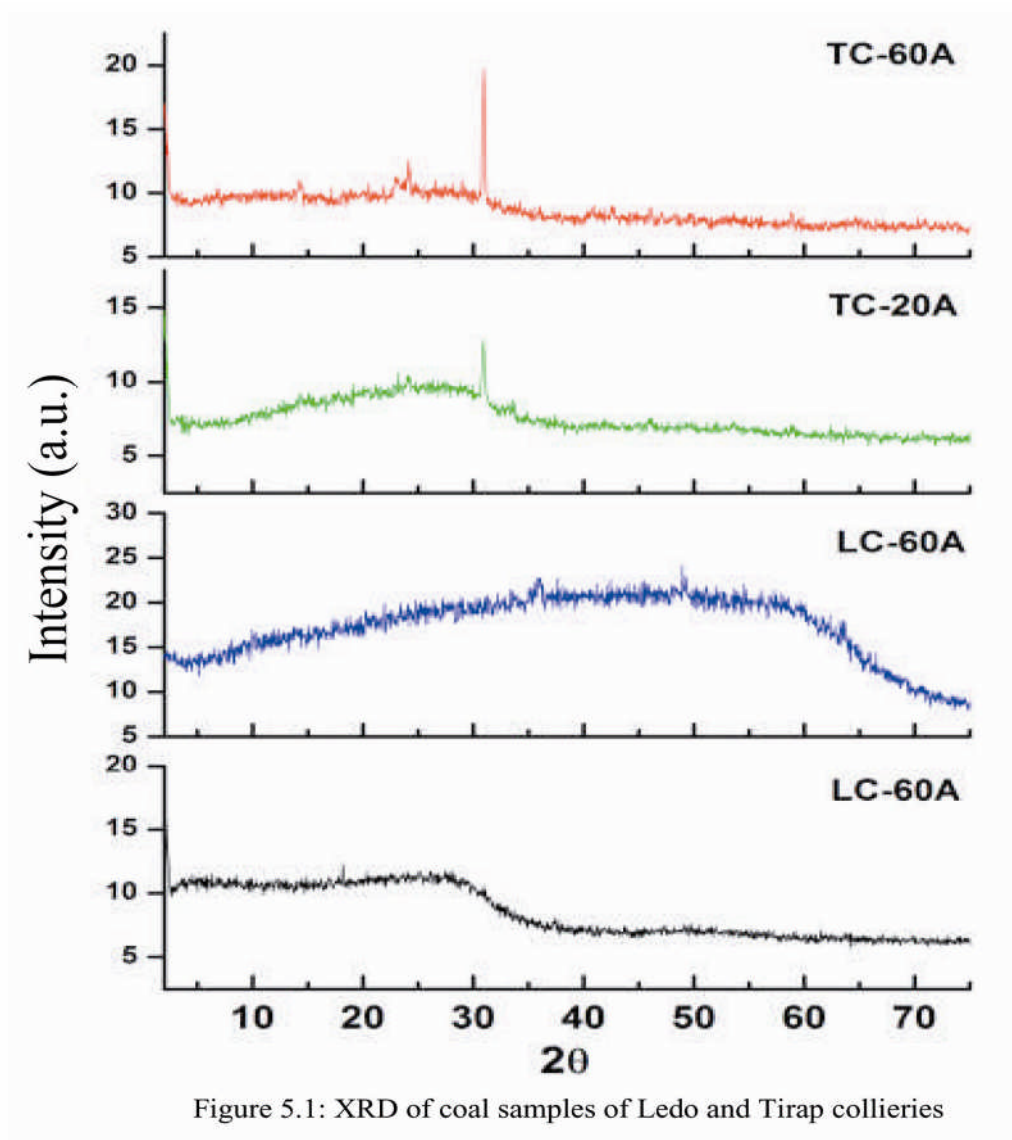
Sample code	F ⁻	Cl ⁻	Br ⁻	NO ₃ ⁻	PO ₄ ³⁻	SO ₄ ²⁻
TC-60A	0.081	0.645	bdl	212.55	0.004	368.85
TC-20A	bdl	0.233	bdl	4.026	bdl	63.71
LC-60A	0.173	0.294	bdl	0.516	bdl	499.30
LC-20A	0.131	0.589	bdl	32.58	1.589	1243.50
LOB-15A	0.043	0.327	bdl	0.475	bdl	125.85
LOB-15B	0.089	0.363	bdl	0.381	bdl	29.73
TOB-15A	0.069	0.794	bdl	196.70	bdl	147.60
TOB-15B	bdl	0.562	bdl	0.441	bdl	27.02
LS-15A	0.331	0.585	bdl	0.526	bdl	28.70
LS-15B	0.011	0.634	bdl	0.334	bdl	11.24
LSE-15A	bdl	1.045	bdl	5.421	bdl	175.00
LSE-15B	0.003	1.224	bdl	20.287	bdl	309.90

Table 5.10 clearly shows that the concentration of Br⁻ in all samples were below detection limit (bdl). This indicates that these values were very low in coal, OB, soil, and sediment samples in comparison to mine water samples (Table 5.8 and Table 5.9). From literature (Bing and Dai, 2011), it is revealed that bromine can easily leached out from coal at a low pH and enter into surrounding soil and surface water, resulting in increase of bromine content in the environment. On the other hand, high concentrations of nitrate ion observed in coal, OB, soil, and sediment samples are may be due the oxidation of organically bound nitrogen.

5.3.5 XRD mineralogy of coal, OB, soil, and sediment

X-ray diffraction analyses of coal, OB, soil and sediment samples were carried out to determine the mineral types and crystallinity of the samples. Figure 5.1, Figure 5.2, and Figure 5.3 show the XRD-mineralogy of coal, OB, soil and sediment distinctly. The assessment of the XRD mineralogical peaks for the presence of minerals in the samples was carried out with the help of the literature available (Saikia et al.,2009a; Saikia

et al.,2009b; Saikia et al.,2015a; Saikia et al., 2016). Quartz is the common mineral present in all the samples and the most prominent peak in all coal samples are due to quartz. The other minerals present are hematite, pyrite, and marcasite. A prominent peak of quartz is due to its high stability. Table 5.11 shows the assignment of d-values for the minerals present in the samples.



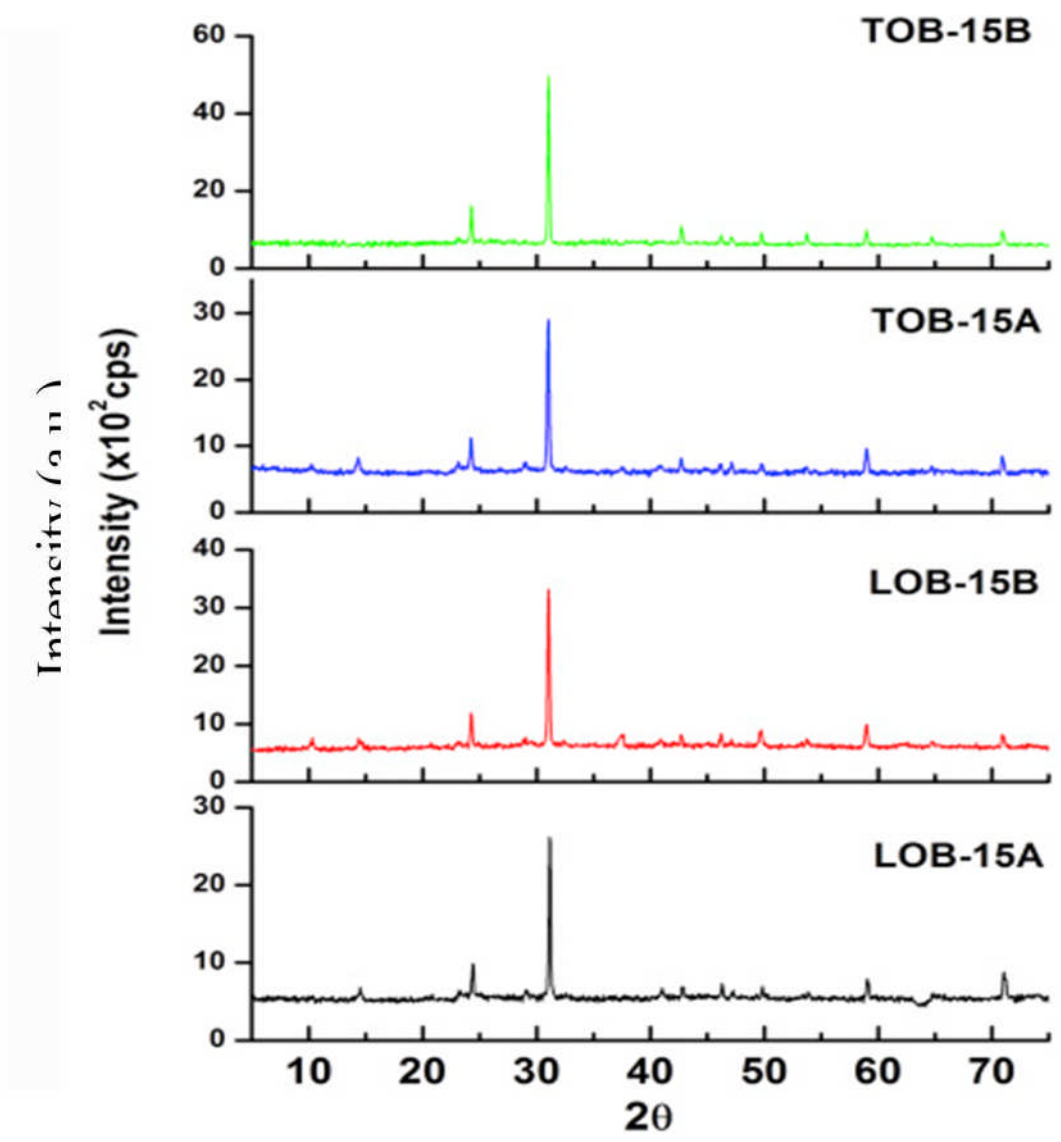


Figure 5.2: XRD of OB samples of Ledo and Tirap collieries

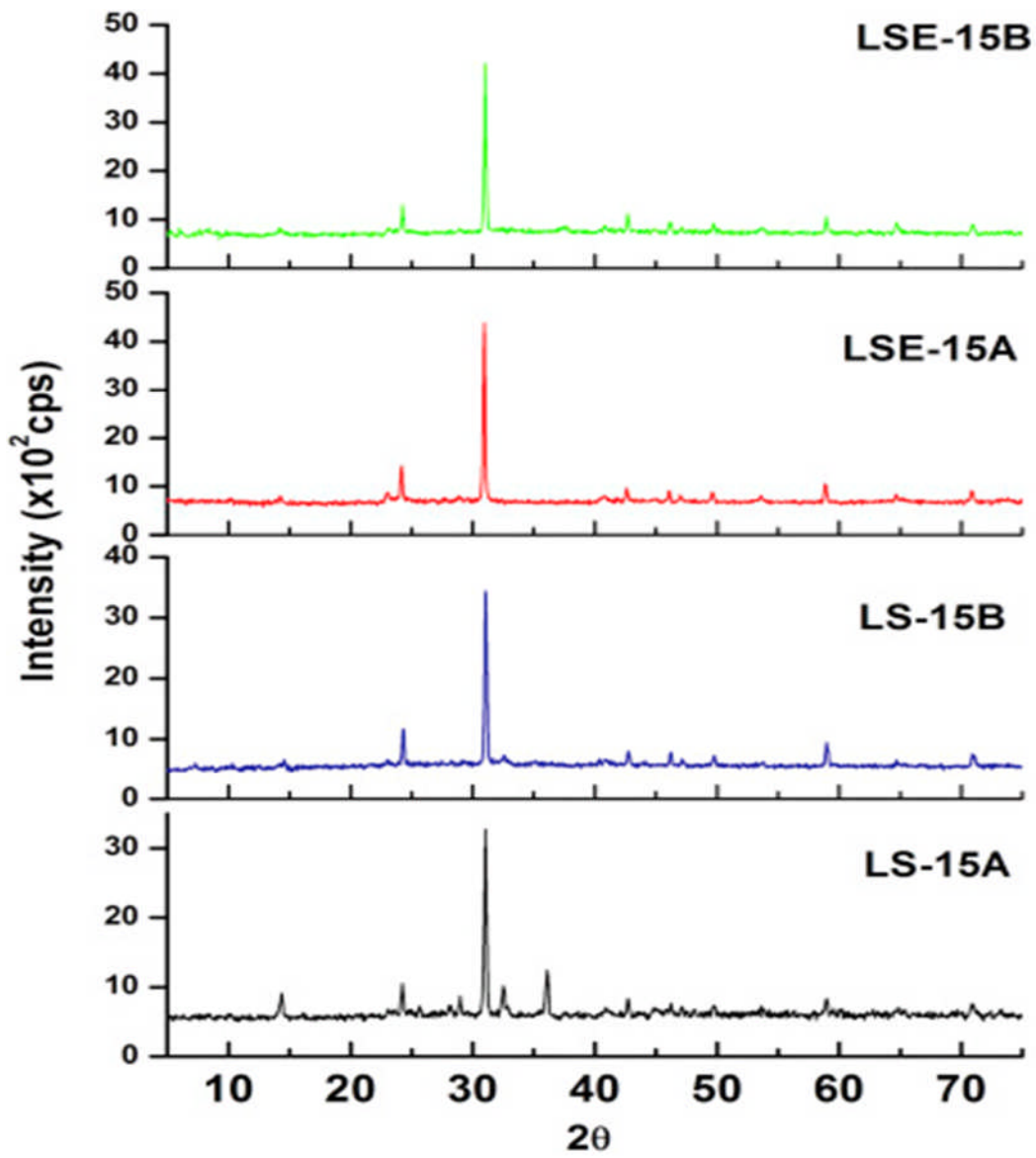


Figure 5.3: XRD of soil and sediment samples of Ledo and Tirap collieries

Table 5.11: Assignments of d-values for the mineral phases

Sample types	d-values	Assessment of mineral phases
Coals (LC-20A, LC-60A, TC-20A, TC-60A)	3.3404	quartz
	1.5789	hematite, quartz
Overburdens (LOB-15A, LOB-15B, TOB-15A, TOB-15B)	3.3404	quartz
	1.8252	quartz, hematite, pyrite,
	2.2801	marcasite
	2.4669	hematite, quartz
	1.5789	quartz, pyrite hematite, quartz
Soil and sediments (LS-15A,LS-15B, LSE-15A, LSE-15B)	4.2654	quartz
	3.3404	quartz
	1.5789	hematite, quartz
	2.4469	quartz, pyrite
	1.8706	quartz, marcasite, hematite
	4.2654	quartz

5.3.6 FTIR analyses of coal, OB, soil, and sediment

The FTIR analysis of the collected samples provides information about the different functional groups as well as other bond stretching bands. The peaks corresponding to the respective functional groups found in coal, OB and soil are shown in Figure 5.4, 5.5, and 5.6. The bands due to stretching vibration of S-S and C-S bonds in primary and secondary thiols were found in the region of 530 and 670 cm^{-1} (Saikia et al. 2009a; Saikia et al., 2009b). The absorption bands due to aliphatic alcohol, ether groups (O-H, C-O-C) and SO_4^{2-} group were found in the region of 1100.1–1005.0 cm^{-1} . The aliphatic amino (NH), aromatic C=C, and aliphatic alkyl groups showed the absorption bands within the range of 1440–1611 cm^{-1} . The aromatic C=C stretching vibrations (1635–1600 cm^{-1})

caused strong absorptions which indicate the presence of more carbon content (Balachandran, 2014). The absorption bands of S-S and C-S groups are of very low intensity and less prominent because the IR absorption bands of organic sulphur groups are very weak, even in high organic sulphur coals (Filippis and Scarsella, 2003). The S-S and C-S, C_{al}-O-C_{al} and SO₄²⁻ bonds are more prominent in Ledo coal (LC-20A) than Tirap colliery indicating high sulphur content (organic and inorganic) in Ledo colliery. Thus the possibility of CMD formation is more in Ledo colliery which increases the amount of deterioration of water quality of nearby water resources.

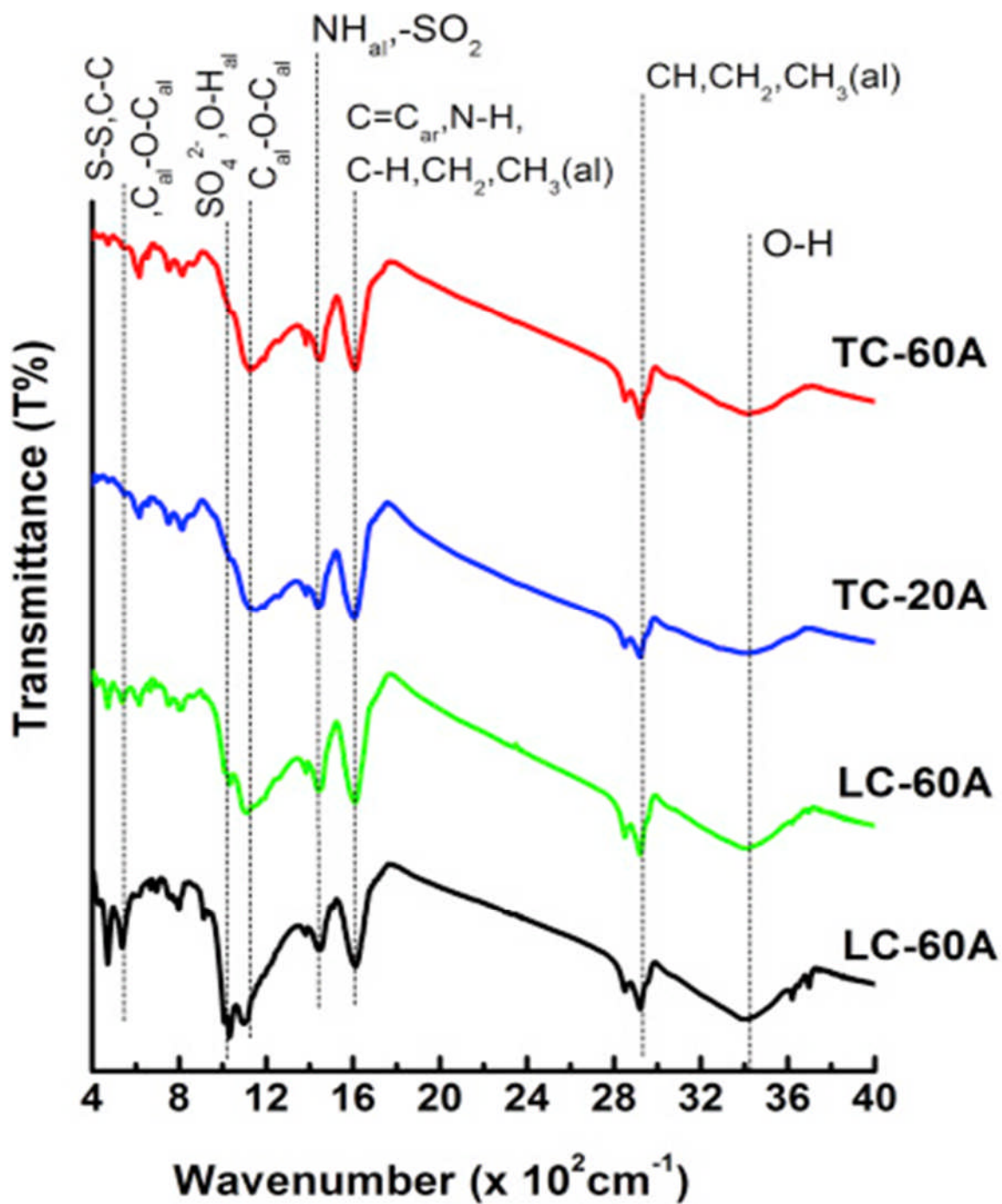


Figure 5.4: FTIR spectra of coal samples of Ledo and Tirap collieries

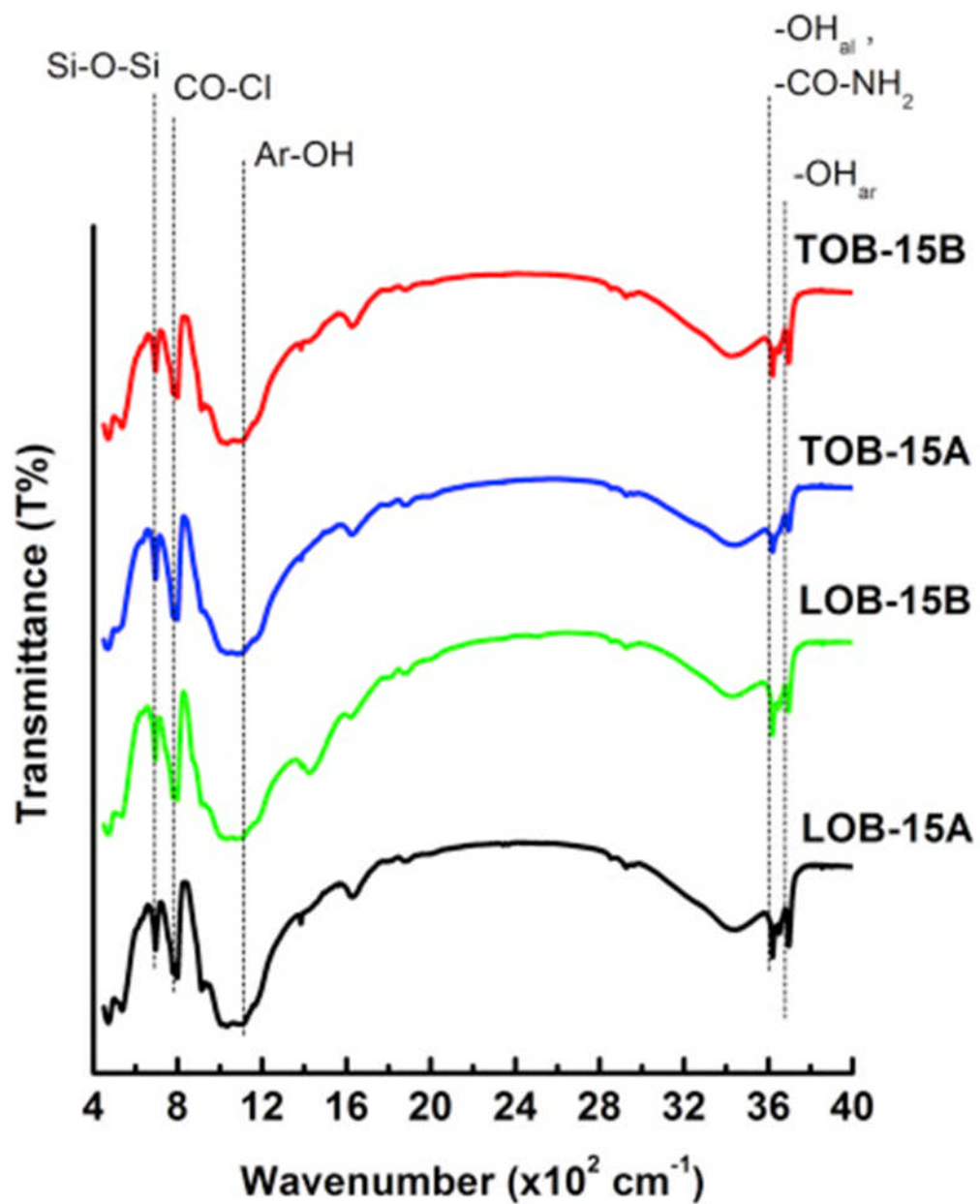


Figure 5.5: FTIR spectra of OB samples of Ledo and Tirap collieries

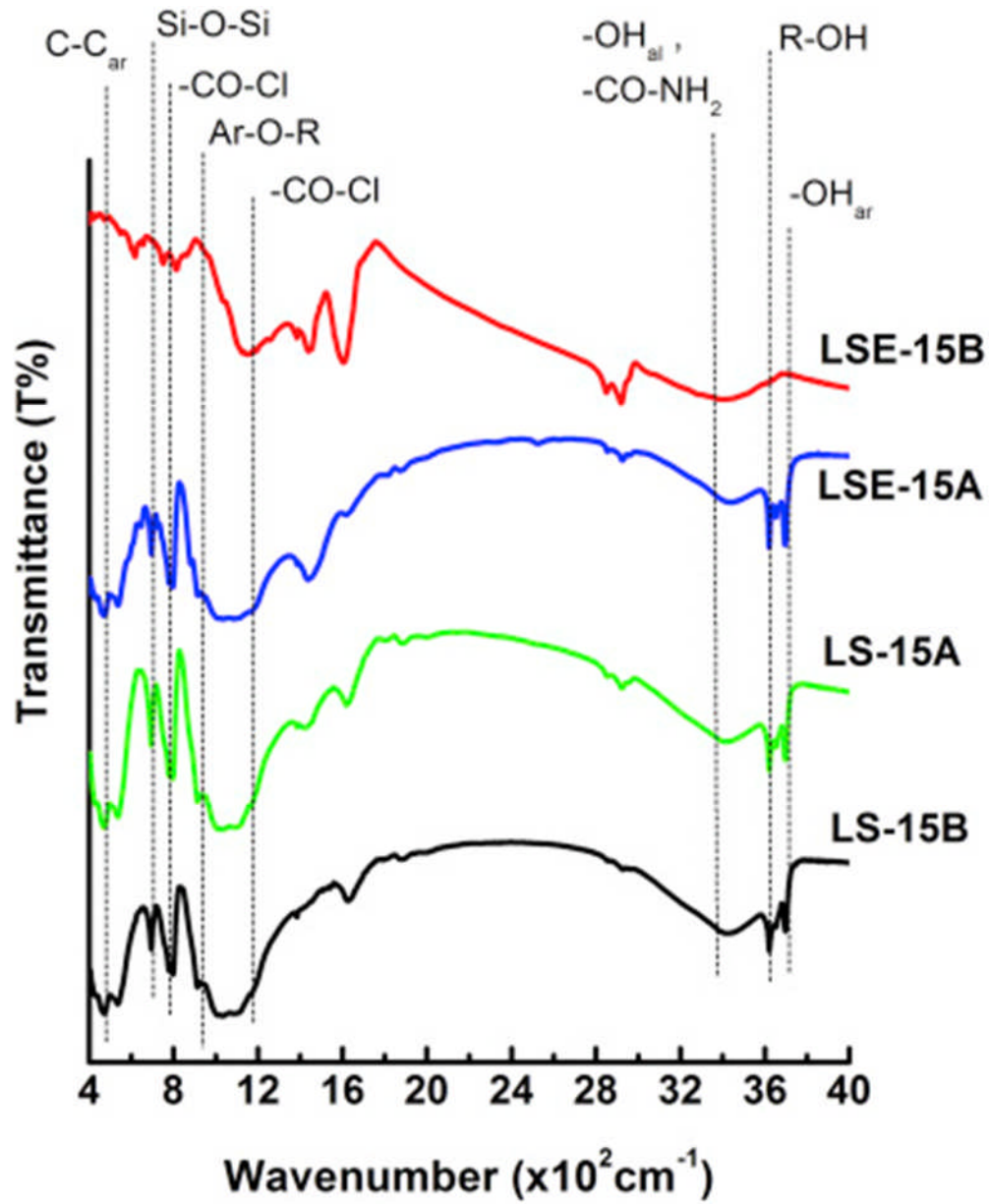


Figure 5.6: FTIR spectra of soil and sediment samples of Ledo and Tirap collieries

Both FTIR and Ion Chromatography analyses show the high concentration of SO_4^{2-} ion in the collected coal, sediment, soil and water samples. In the FTIR analyses the prominent band for SO_4^{2-} ion indicates its high concentration.

5.3.7 Raman analysis of coal, overburden, soil, and sediment

Raman spectroscopy is used for the characterization of carbon minerals. Raman spectra of four different coals from Ledo and Tirap collieries were recorded with an excitation wavelength of 542 nm. Figures 5.7, 5.8, and 5.9 show the Raman bands of NER coal, overburden, soil and sediment respectively. In this analysis, two distinct peaks were observed at around 1348 and 1589 cm^{-1} . The Raman band occurring at 1589 cm^{-1} is interpreted as the peak related to the graphite band which is observed at wavelength 1580 cm^{-1} . The graphite band has been assigned as a G band (Tsu et al., 1977). Thus the band at 1589 cm^{-1} has E_{2g} symmetry which involves in plane bond-stretching vibration of all pairs of sp^2 atoms both in rings and chains. This occurs in all sp^2 sites and it is observed within the range of 1500-1630 cm^{-1} . The band found at 1348 cm^{-1} is attributed to the structural disorder which is designated as D-band (Lin-Vien et al., 1991). Presence of this band indicates the presence of defect in graphite structure. However, the presence of D and G bands indicates the graphite nature in North-eastern coal.

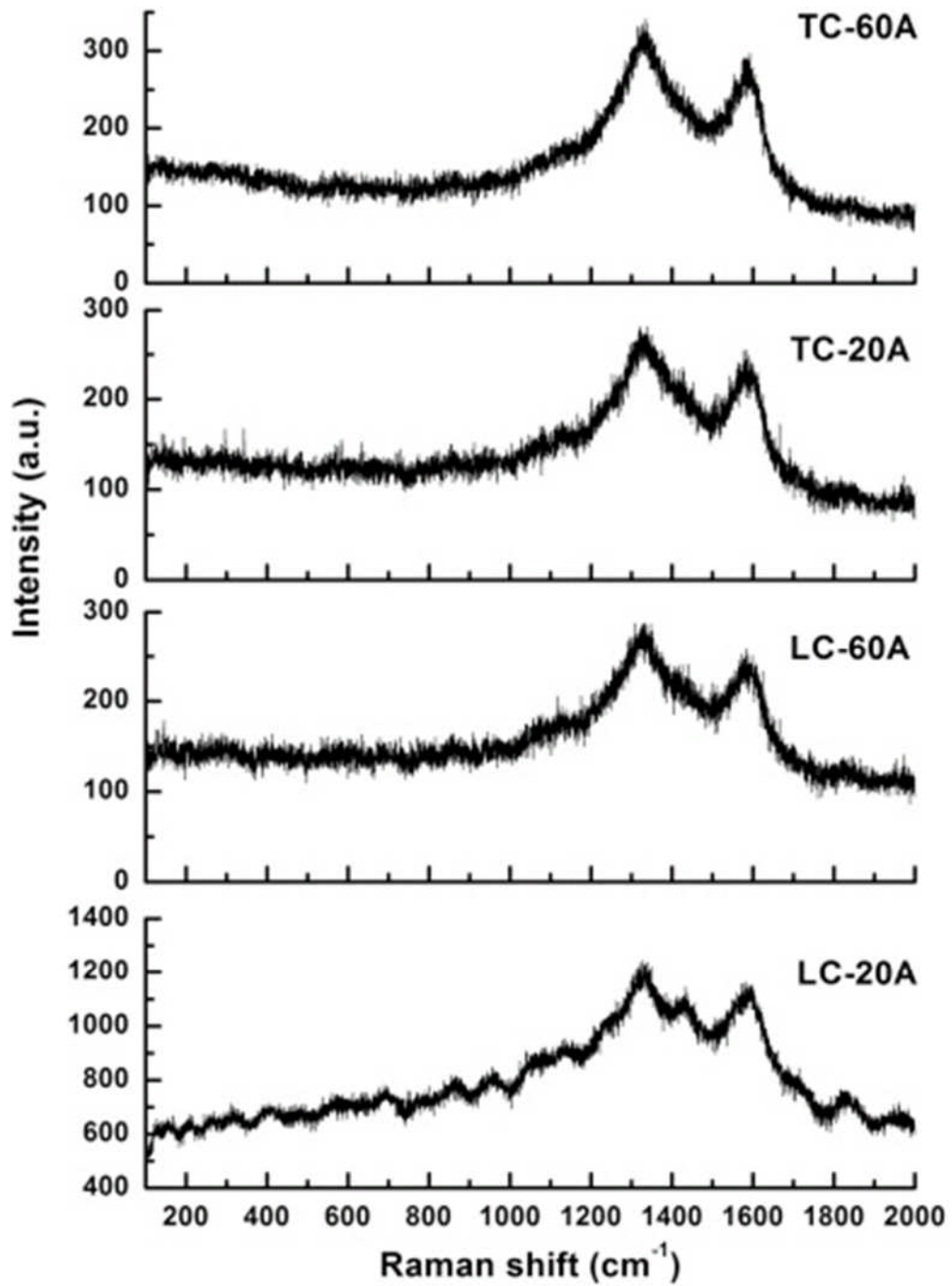


Figure 5.7: Raman spectra of coal samples of Ledo and Tirap collieries

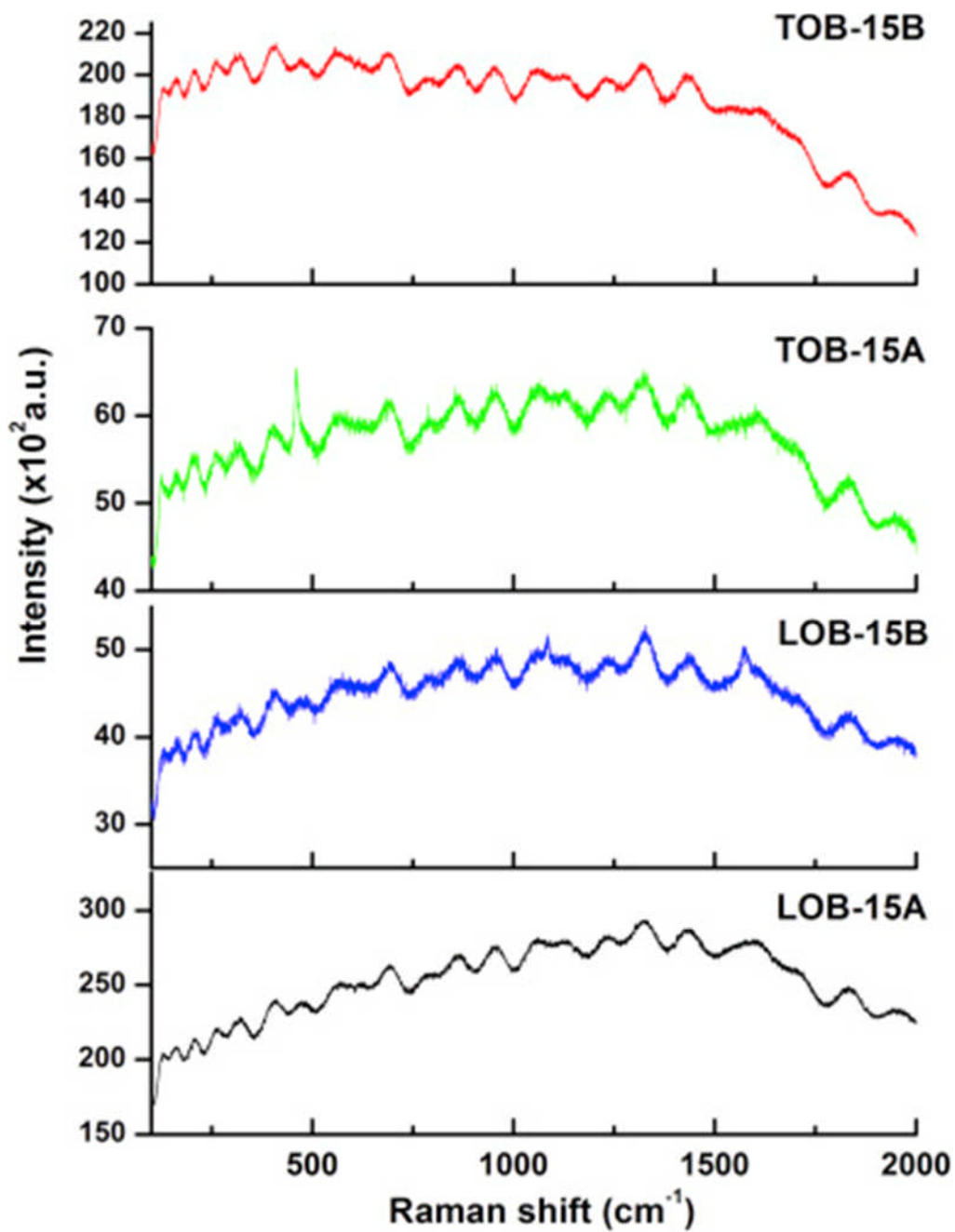


Figure 5.8: Raman spectra of OB samples of Ledo and Tirap collieries

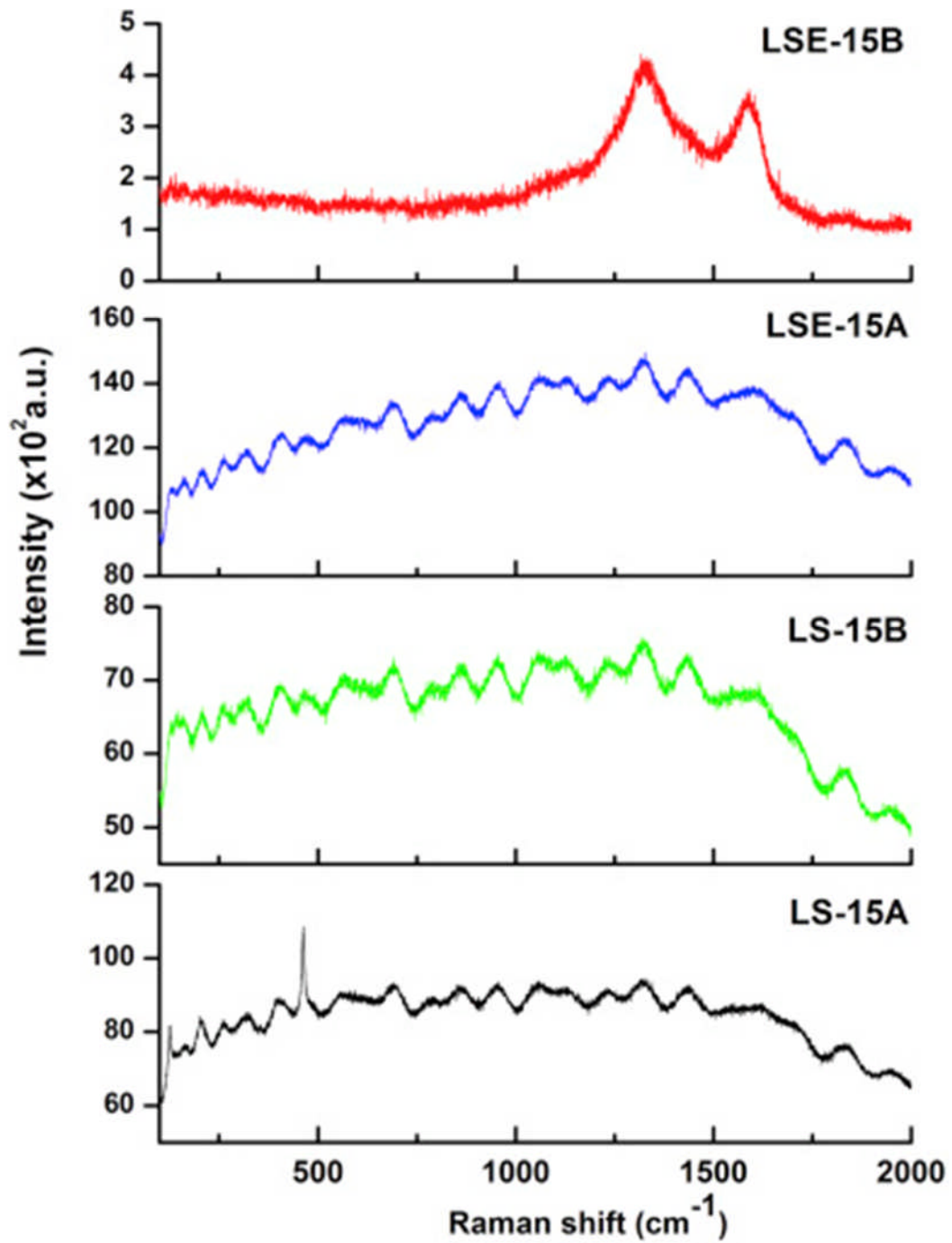


Figure 5.9: Raman spectra of soil and sediment of Ledo and Tirap collieries

5.3.8 Mössbauer spectroscopic analyses of coal, OB, soil, and sediment

The ^{57}Fe Mössbauer spectra of coal, overburden and soil/sediment samples were measured in order to obtain information about the iron containing minerals present in them. Pyrite was found to be the only Fe-mineral present in coal, indicated by the 100% relative abundance, as shown in Table 5.10. In the XRD analyses hematite was also observed but in a Mössbauer spectrum hematite was observed as a sextet with a hyperfine magnetic field of about 50 T. In the present investigation only doublets and no sextets were observed, thus excluding the presence of hematite in the Mössbauer results. In most of the overburden and soil or sediment samples pyrite was present in various amounts. The overburden sample from the Ledo coal mine (LOB-15B) contain lowest amount of pyrite (less than 10%). Other Fe-minerals present in the overburden and soil, and sediment samples include illite $(\text{K,H}_2\text{O})(\text{Al,Mg,Fe})_2(\text{Si,Al})_4\text{O}_{10}[(\text{OH})_2\cdot(\text{H}_2\text{O})]$, jarosite and marcasite. Jarosite and iron sulphate (in overburden and soil and sediment samples, Table 10) are oxidation products of pyrite. Minerals such as illite normally appear in a XRD spectrum at very small angles and thus could not be detected in the XRD spectra, but were found in the Mössbauer spectra (Table 5.12). The high relative abundance of pyrite in the coal samples indicates the higher possibility of CMD formation.

Table 5.12: Mössbauer parameters of Fe-components observed in the samples

Sample	Sample code	Component	IS mms^{-1} (± 0.01)	QS mms^{-1} (± 0.01)	H Tesla (± 0.3)	Relative intensity (%)
Coal	LC-20A	Pyrite	0.36	0.73	–	100
	LC-60A	Pyrite	0.37	0.62	–	100
	TC-20A	Pyrite	0.32	0.64	–	100
	TC-60A	Pyrite	0.33	0.64	–	100
Overburden	LOB-15A	Pyrite/marcasite	0.35	0.54	–	61
		Illite	1.05	2.41	–	29
	LOB-15B	Pyrite	0.31	0.60	–	8
		Illite	1.22	1.98	–	92
	TOB-15A	Jarosite	0.31	0.65	–	68
		Illite	1.21	1.92	–	32
	TOB-15B	Pyrite	0.34	0.60	–	87
		Iron sulphate	1.27	2.40	–	13
Soil and sediment	LS-15A	Pyrite	0.32	0.57	–	10
		Illite	1.22	1.84	–	90
	LS-15B	Pyrite	0.34	0.67	–	56
		Iron sulphate	1.12	2.65	–	44
	LSE-15A	Pyrite/Marcasite	0.33	0.56	–	87
		Iron sulphate	1.16	2.34	–	22
	LSE-15B	Pyrite	0.31	0.66	–	72
		Illite	1.20	1.88	–	28

Note: IS = Isomer shift relative to α -Fe, QS = Quadrupole splitting, H = Hyperfine magnetic field strength

5.3.9 Observation from EF-SEM and HR-TEM analyses of coal and OB

The nano-mineralogical analysis of coal and overburden revealed the presence of Si minerals like kaolinite $[\text{Al}_2\text{Si}_2\text{O}_5(\text{OH})_4]$ with other minerals including sulphate minerals such as barite $[\text{BaSO}_4]$, jarosite $[\text{KFe}_3(\text{SO}_4)_2(\text{OH})_6]$, pickeringite $[\text{MgAl}_2(\text{SO}_4)_4 \cdot 22(\text{H}_2\text{O})]$ sulphide mineral galena $[\text{PbS}]$, pyrite $[\text{FeS}_2]$, oxide mineral hematite $[\text{Fe}_2\text{O}_3]$, and organic matters which are combined with pyrite (Figure 5.10). These minerals were also common in Brazilian (Cutruneo et al., 2014) and Chinese coal (Yang et al., 2015). HR-TEM analyses (Figure 5.11) of the coal and mine overburden reveals the presence of nano-minerals containing potentially hazardous elements.

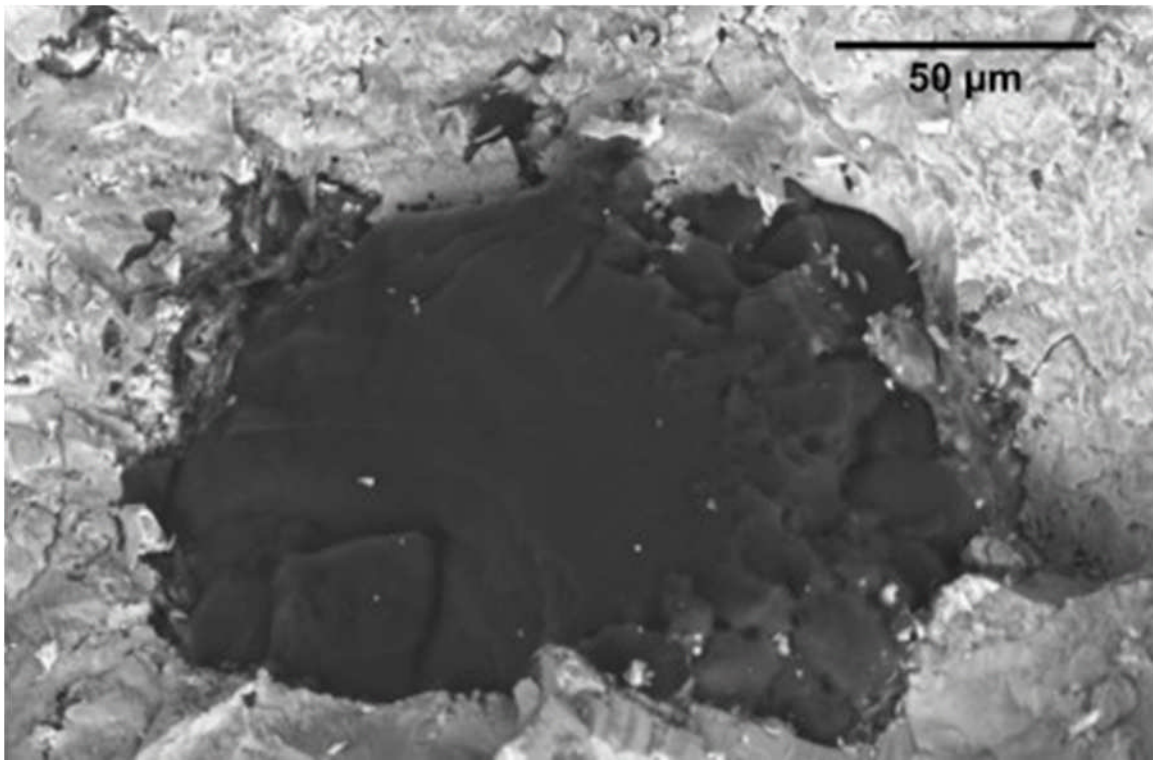


Figure 5.10: FESEM image showing Organic Matter “Inside or below” of the pyrite (LC- 20A sample) (secondary electron image)

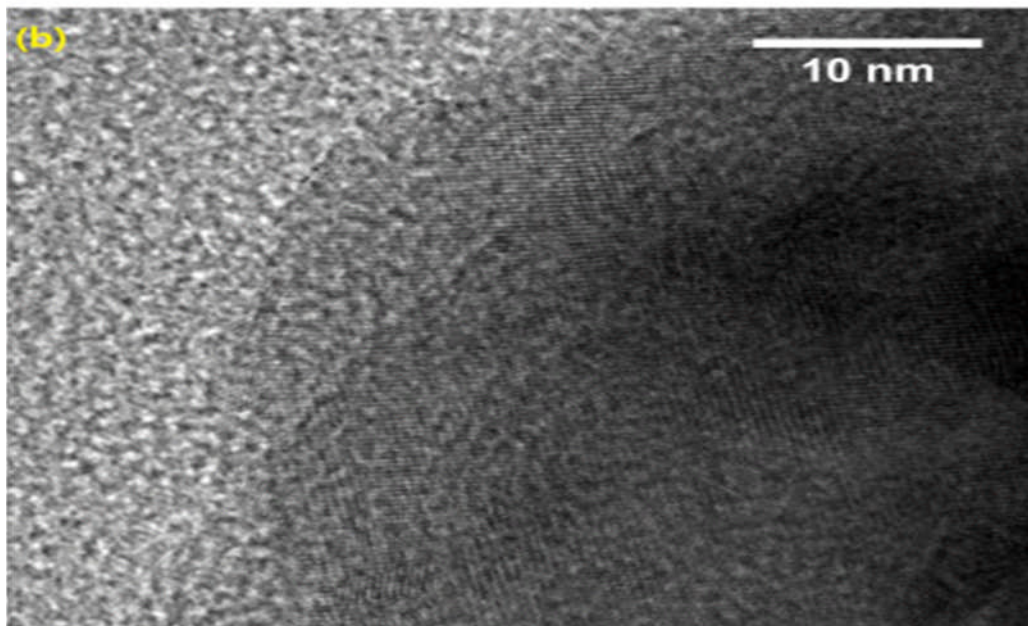
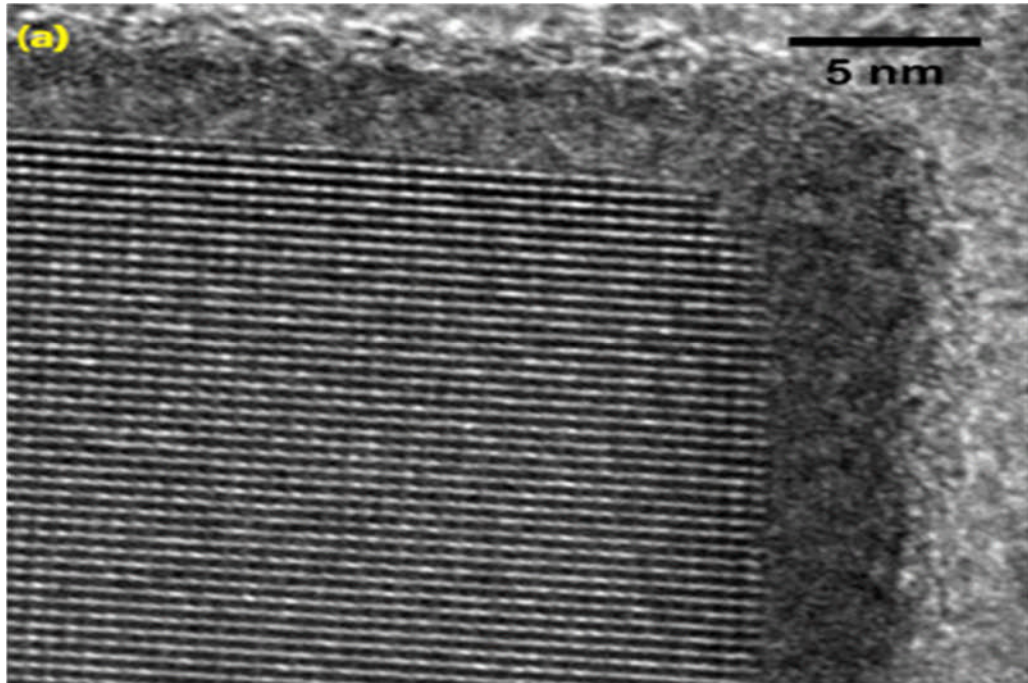


Figure 5.11: HRTEM images of Jarosite (a) and Amorphous and crystalline mixed carbonaceous matter contain hazardous elements (b) (LOB-15B)

The overburden materials occur both in amorphous and crystalline forms containing hazardous elements. Galena containing high proportions of Pb, kaolinite containing high concentrations of Al and Si can lead to health implications (Figure 5.12).

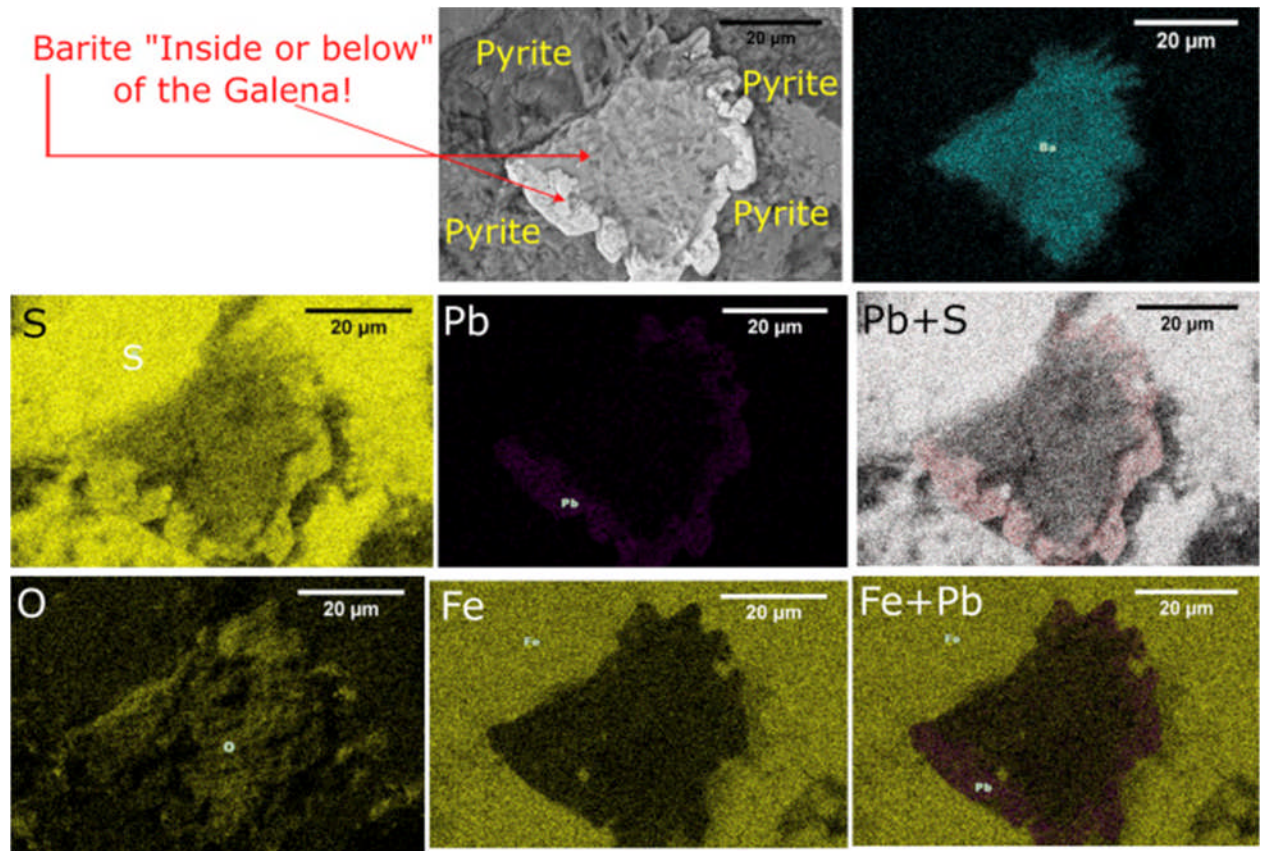


Figure 5.12: FESEM of coal sample (LC-20A sample) (secondary electron image)

The sulphate minerals like barite, jarosite, pickeringite analysed by FE-SEM are the primary sources of AMD formation. The presence of nano-hematite in coal samples was revealed by HR-TEM technique (Figure 5.13). These nano-hematites have high surface area and high reactivity, making them environmentally sensitive. Studies have

shown that the concentrations of various metals in the soils increase with decreasing particle size (Al-Rajhi et al., 1996; Ljung et al., 2006; Hower et al., 2008).

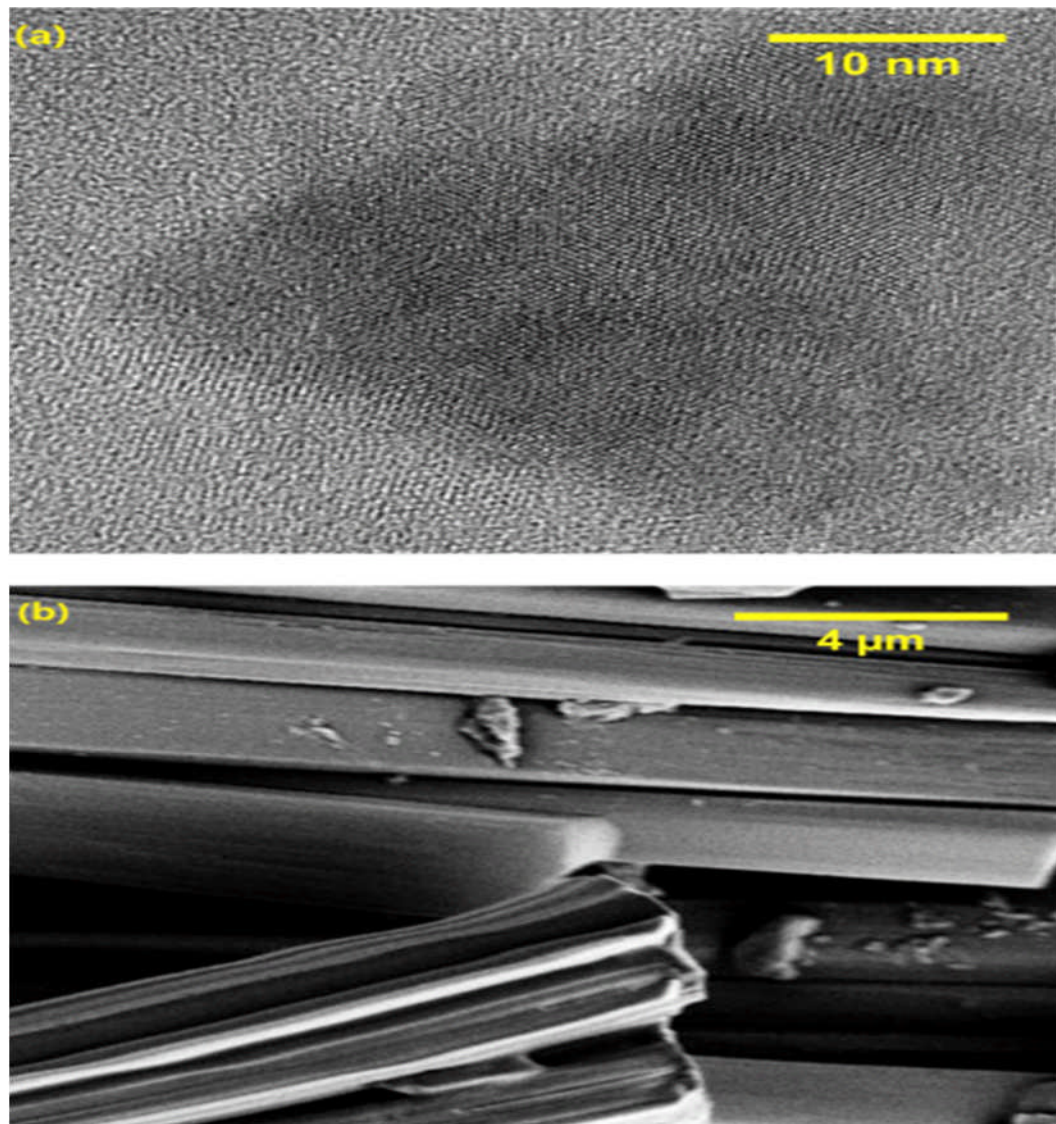


Figure 5.13: TEM image of singular nano-hematite (a) and FESEM image of Pickeringite in LC-20A (b)

Studies relating to nano-toxicity indicate that particle size and the properties linked to the particle size, has an effect on both the bioavailability and the subsequent level of toxicity to organisms including human being. In some aquatic organisms, various nanoparticles like SiO_2 , ZnO_2 have been reported to cause adverse effect such as acute toxicity, bio-modification, reproductive alteration and behavioural and physiological changes (Baun et al., 2008). The XRD, FE-SEM and HR-TEM analyses confirmed the mineral jarosite in combination with kaolinite and gypsum in coal as well as mine rejects (Figure 5.14). Further, most of the minerals present in the samples are sulphate minerals which are shown also in ion chromatographic analysis. The jarosite phase is environmentally important because its structure readily takes up Pb (Stoffregen et al., 2000).

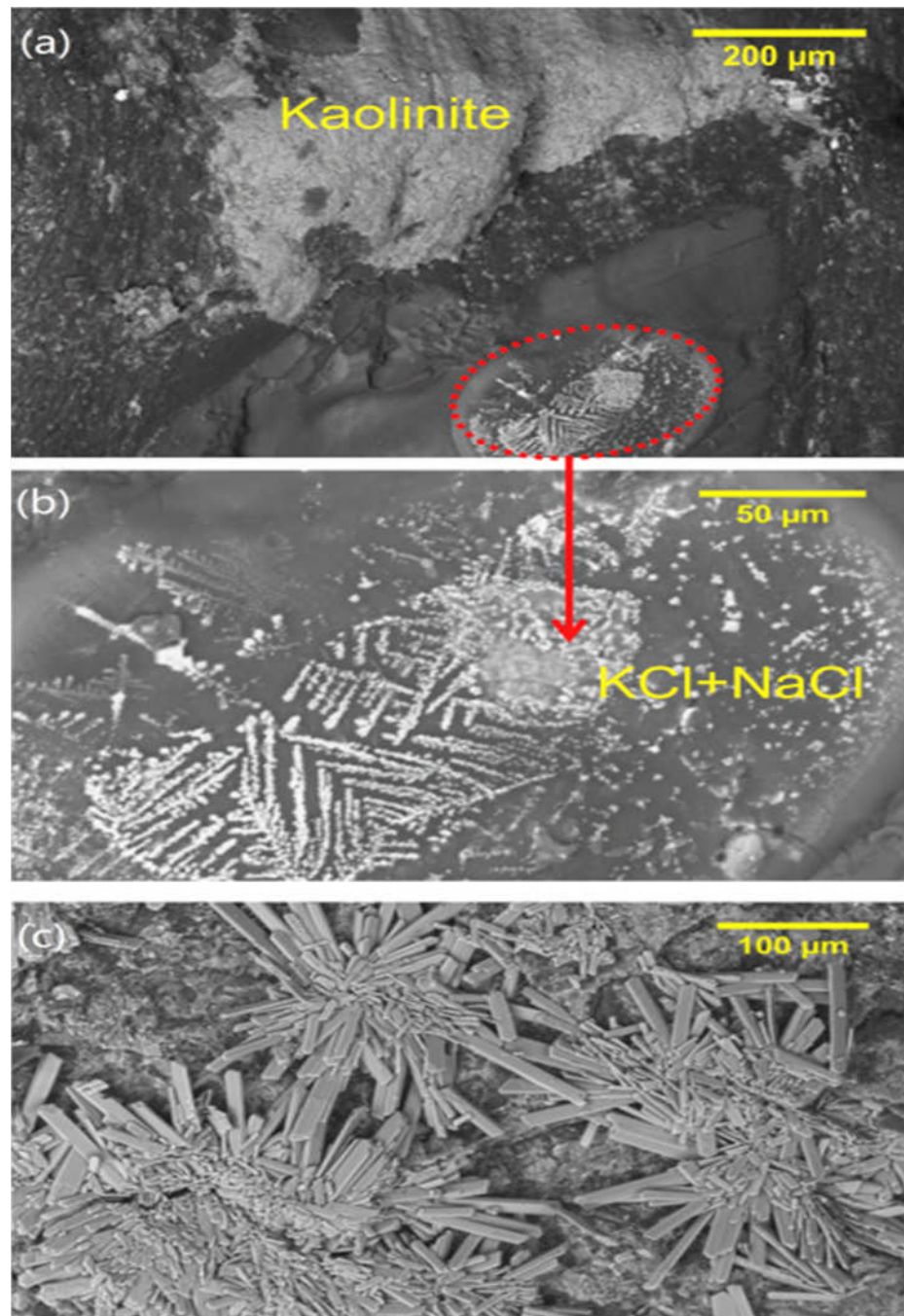


Figure 5.14: Kaolinite (a), NaCl + KCl (b) and gypsum (c) in LOB-15A sample (secondary electron image)

5.3.10 Mobility of elements in AMD water

FE-SEM, HR-TEM, XRD and ion chromatographic analyses confirm the presence of most of the elements in coal, overburden, soil and sediment samples some of which are hazardous to life as well as to plant kingdom. These elements include S, Cl, Br, F, Si, Al, Fe, Mg, Pb, Ca, As, and Ba. The amount of impact of these elements depends on their mobility in AMD water which can contaminate water bodies and soil nutrition. The excavation of coal exposes the sulphide minerals to the atmosphere and their oxidation leads to the generation of highly acidic (low pH) mine drainage. Due to its acidic nature, AMD can dissolve various metals. Subsequent dilution and interaction with different minerals, specially carbonates increase the pH of AMD and there is the formation of the typical orange–red–yellow precipitate of ferric hydroxide (Alpers and Blowers, 1994). The ferric hydroxide precipitated from AMD water plays a vital role in controlling the mobility of metals through scavenging and/or releasing elements under varying physicochemical conditions (Chapman et al., 1983, Cornell and Schwertmann, 2006). The low pH of AMD allows metals to be more mobile than under neutral conditions (Stumm and Morgan, 1996). Metal concentrations in AMD from coal mines are controlled by three factors: (1) oxidation rate of pyrite, (2) mineralogy of country rock, (3) pH of leachate (Yue and Zhao, 2008). At low pH levels, the toxic (heavy) metals are more soluble. There are also secondary reactions between iron sulphates, sulphuric acid and the compounds in clays (kaolinite), sandstones, limestone, sulphides and various organic substances present in coal mine drainage or streams. This leads to the presence of Ca, Mg, Al, Na, K, Mn, Pb, As etc. in coal mine drainage (Rawat and Singh, 1983). The presented data of the minerals and nano-particles present shows their ability to control the mobility of hazardous elements, suggesting possible use in environmental management technology, including restoration of the delicate Indian coal mine areas.

References

- Al-Rajhi, M.A., Al-Shayeb, S.M., Seaward, M.R., Edwards, H.G., 1996. Particle size effect for metal pollution analysis of atmospherically deposited dust. *Atmospheric Environment* 30 (1), 145-153.
- ASTM D2492-02, Standard Test Method for Forms of Sulfur in Coal (www.astm.org).
- Balachandran, M., 2014. Role of infrared spectroscopy in coal analysis- an investigation. *American Journal of Analytical Chemistry* 5, 367-372.
- Baruah, B.P., Saikia, B.K., Kotoky, P., Rao, P.G., 2006. Aqueous leaching on high Sulfur Sub-bituminous coals, in Assam, India. *Energy and Fuels* 20 (4), 1550-1555.
- Baun, A., Hartmann, N.B., Grieger, K., Kusk, K.O., 2008. Ecotoxicity of engineered nano-particles to aquatic invertebrates: a brief review and recommendations for future toxicity testing. *Ecotoxicology* 17, 387-395.
- Beaulieu, D., 2018. Soil pH: What It Means and Why It Matters. The Spruce.
- Bing-xian, PENG., Dai-she, W.U., 2011. Leaching characteristics of bromine in coal. *Jour of Fuel Chem and Technol* 39(9), 647-651.
- Civeira, S. Matheus., Ramos, G. Claudete., Oliveira, L.S. Marcos., Kautzmann, M. Rubens ., Taffarel, R. Silvio., Teixeira, C. Elba ., Silva, F.O. Luis., 2016. Nano-mineralogy of suspended sediment during the beginning of coal rejects spill. *Chemosphere* 145,142-147]
- Chon, H.T., Hwang, J.H., 2000. Geochemical characteristics of the acid mine drainage in the water system in the vicinity of the Dogye coalmine in Korea. *Environmental Geochemistry and Health* 22, 155-172.
- Cutruneo, C.M., Oliveira, M.L., Ward, C.R., Hower, J.C., de Brum, I.A., Sampaio, C.H., Kautzmann, R.M., Taffarel, S.R., Teixeira, E.C., Silva, L.F.O., 2014. A mineralogical and geochemical study of three Brazilian coal cleaning rejects: demonstration of electron beam applications. *International Journal of Coal Geology* 130, 33-52.

- Dutta, M., Saikia, J., Taffarel, S.R., Waanders, F.B., Medeiros, D.; Cutruneo, C.M.N.L., Silva, L.F.O., Saikia, B.K., 2017. Environmental assessment and nano-mineralogical characterization of coal, overburden and sediment from Indian coal mining acid drainage. *Geoscience Frontiers* 8(6), 1285-1297.
- Farre, M., Sanchís, J., Barcel, O.D., 2011. Analysis and assessment of the occurrence, the fate and the behavior of nano-materials in the environment. *Trends Anal. Chem.* 30, 517-527.
- Filippis, P.D., Scarsella, M., 2003. Oxidative desulfurization: oxidation reactivity of the sulfur compounds in different organic matrixes. *Energy & Fuels* 17, 1452-1455.
- Finkelman, R.B., 1994. Modes of occurrence of potentially hazardous elements in coal: Levels of confidence. *Fuel Processing Technology* 39, 21.
- Finkelman, R.B., 1995. Modes of occurrence of environmentally-sensitive trace elements in coal. *Environmental Aspects of Trace Elements in Coal* (Eds. D.J. Swaine and F. Goodarzi). pp 24-50.
- Gaur, N., Bhardwaj, V., Rathi, M., 2014. Health risks of Engineered Nanoparticles. *Int J Curr Microbiol App Sci* 3(7), 132-147.
- Hower, J.C., Graham, U.M., Dozier, A., Tseng, M.T., Khatri, R.A., 2008. Association of the heavy metals with nanoscale carbon in a Kentucky electrostatic precipitator. *Environmental Science & Technology* 42 (22), 8471-8477.
- Hower, J.C., O'Keefe, J.M.K., Henke, K.R., Wagner, N.J., Copley, G., Blake, D.R., Garrison, T.M., Oliveira, M.L.S., Kautzmann, R.M., Silva, L.F.O., 2013. Gaseous emissions from the Truman Shepherd coal fire, Floyd County, Kentucky: a re-investigation following attempted mitigation of the fire. *Int J Coal Geol* 116–117, 63–74.
- Leeuwen, V., Rolaf, F.X., Sangster, B., 1988. The toxicology of bromide ion. *CRC Critical Reviews in Toxicology* 18 (3), 189-215.
- Leon-Mejia, G., Espitia-Perez, L., Hoyos-Giraldo, L.S., Da Silva, J., Hartmann, A., Henriques, J.A., Quintana, M., 2011. Assessment of DNA damage in coal open-

- cast mining workers using the cytokinesis-blocked micronucleus test and the comet assay. *Sci Total Environ* 409, 686–691.
- Lin-Vien, D., Colthup, N.B., Fateley, W.G., Grasselli, J.G., 1991. *The Handbook of Infrared and Raman Characteristic Frequencies of Organic Molecules*. New York.
- Ljung, K., Selinus, O., Otabbong, E., 2005. Metals in soils of children's urban environments in the small northern European city of Uppsala. *Science of the Total Environment* 366 (2-3), 749-759.
- Ljung, K., Selinus, O., Otabbong, E., Berglund, M., 2006. Metal and arsenic distribution in soil particle sizes relevant to soil ingestion by children. *Appl Geochem* 21, 1613–1624.
- Luis F.O. Silva., Macias, F., Marcos, L.S. Oliveira., M. Kátia da Boit., Frans, Waanders., 2011. Coal cleaning residues and Fe-minerals implications. *Environ Monit Assess* 172, 367–378.
- Mackay, C.E., Johns, M., Salatas, J.H., Bessinger, B., Perri, M., 2006. Stochastic probability modeling to predict the environmental stability of nanoparticles in aqueous suspension. *Integr. Environ Assess Manag* 2, 293-298.
- Matheus S. Civeira , Claudete G. Ramos , Marcos L.S. Oliveira , Rubens M. Kautzmann , Silvio R. Taffarel , Elba C. Teixeira , Luis F.O. Silva , 2016. Nano-mineralogy of suspended sediment during the beginning of coal rejects spill. *Chemosphere* 145,142-147.
- Odenheimer, J., Skousen, J., McDonald, L.M., Vesper, D.J., Mannix, M., Daniels, W.L., 2015. Predicting release of total dissolved solids from overburden material using acid-base accounting parameters. *Geochemistry: Exploration, Environment Analysis* 15 (2-3), 131-137.
- Saikia, B.K., Boruah, R.K., Gogoi, P.K., 2009. X-ray (radial distribution function, RDF) and FT-IR analysis of high sulphur Tirap (India) coal. *Journal of the Energy Institute* 82 (2), 106-108.

- Saikia, B.K., Boruah, R.K., Gogoi, P.K., Baruah, B.P., 2009. A thermal investigation on coals from Assam (India). *Fuel Processing Technology* 90, 196-203.
- Saikia, B.K., Ward, Colin R., Oliveira, Marcos L.S., Hower, James C., Baruah, Bimala P., Marcel Braga, Luis F. Silva., 2014. Geochemistry and nano-mineralogy of two medium-sulfur northeast Indian coals. *International Journal of Coal Geology* 121, 26-34.
- Saikia, B.K., Ward, C.R., Oliveira, M.L., Hower, J.C., De Leao, F., Johnston, M.N., O'Bryan, A., Sharma, A., Baruah, B.P., Silva, L.F.O., 2015a. Geochemistry and nano-mineralogy of feed coals, mine overburden, and coal-derived fly ashes from Assam (North-east India): a multi-faceted analytical approach. *International Journal of Coal Geology* 137, 19-37.
- Saikia, J., Narzary, B., Roy, S., Bordoloi, M., Saikia, P., Saikia, B.K., 2016. Nanominerals, fullerene aggregates, and hazardous elements in coal and coal combustion generated aerosols: an environmental and toxicological assessment. *Chemosphere* 164, 84-91.
- Schins, R.P., Borm, P.J., 1999. Mechanisms and mediators in coal dust induced toxicity: a review. *Ann Occup Hyg* 43, 7–33.
- Shahabpour, J., Doorandish, M., Abbasnejad, A., 2005. Mine drainage water from coal mines of Kerman region, Iran. *Environmental Geology* 47 (7), 915.
- Silva, F.O. Luis., Macias, F., · Marcos Oliveira, L.S. Marcos., · Kátia, M. da Boit., Waanders, Frans., 2011. Coal cleaning residues and Fe-minerals implications. *Environ Monit Assess* 172, 367–378.
- Swer, S., Singh, O.P., 2003. Coal mining impacting water quality and aquatic biodiversity in Jaintia Hills District of Meghalaya. *ENVIS Bulletin-Himalayan Ecology* 11 (2), 26-33.
- Tsu, R., Jesus González, H., Isaac Hernández, C., Luengo, C.A., 1977. Raman scattering and luminescence in coal and graphite. *Solid State Communications* 24 (12), 809-812.

- Vogel, A.I., 1969. A Textbook of Quantitative Inorganic Analysis, Including Elementary Analysis. Wiley, New York.
- Wang, X., Qin, Y., Chen, Y., 2006. Heavy metals in urban roadside soils, part 1: effect of particle size fractions on heavy metals partitioning. *Environ Geol* 50, 1061–1066.
- Warheit, D.B., 2004. Nano-particles: health impacts. *Mater Today* 32–35.
- Warheit, D.B., Webb, T.R., Reed, K.L., 2003. Pulmonary toxicity studies with TiO₂ particles containing various commercial coating. *Toxicologist* 72, 298.
- Xiuyi, T. Mineral Matter in Coal, Oil Shale, Natural Bitumen, Heavy Oil and Peat - Volume 1 No. of Pages: 516 ISBN: 978-1-84826-017-7 (eBook) ISBN: 978-1-84826-467-0 (Print Volume).
- Yang, N., Tang, S., Zhang, S., Chen, Y., 2015. Mineralogical and geochemical compositions of the No. 5 coal in Chuancaogedan mine, Junger coalfield, China. *Minerals* 5 (4), 788-800.
- Zamuda, C.D., Sharpe, M.A., 2007. A case for enhanced use of clean coal in India: an essential step towards energy security and environmental protection. Workshop on Coal Beneficiation and Utilization of Rejects. Ranchi, India.